

$$(\tau(\text{LSI}))^{-1} = \tau_0^{-1} + k_g[\text{O}_2] \quad (\text{VII})$$

$k_g = (5 \pm 1) \cdot 10^5 \text{ L/mol s}$  was found, which compares with  $(5.5 \pm 0.5) \cdot 10^5 \text{ L/mol s}$  for the reaction of lateral poly( $\alpha$ -methylstyryl) radicals with  $\text{O}_2$ . By extrapolation of  $\tau^{-1}$  for  $[\text{O}_2] \rightarrow 0$  the lifetime  $\tau_0$  of macroradicals in the absence of oxygen was found as ca.  $4 \times 10^{-3} \text{ s}$ .

At oxygen concentrations greater than about  $1 \times 10^{-3} \text{ mol/L}$  practically all macroradicals have reacted with  $\text{O}_2$ , as is inferred from the fact that the degree of degradation becomes independent of  $[\text{O}_2]$  (see Figure 2). The plots demonstrating the decay of the LSI become curved at higher oxygen concentrations (see Figure 3). A possible explanation is that as the oxygen concentration increases the rate of the reaction  $\text{P} \cdot + \text{O}_2$  becomes faster. Therefore, the cleavage reaction becomes rate determining for the LSI decay at relatively high oxygen concentrations. In other words, at  $[\text{O}_2] \approx 10^{-5} \text{ mol/L}$   $v_g = k_g[\text{O}_2][\text{P} \cdot] < v_i = k_i[\text{PO}_2 \cdot]$  and at  $[\text{O}_2] \approx 10^{-3} \text{ mol/L}$   $v_g > v_i$ . This conclusion is supported by the fact that an increase of  $[\text{O}_2]$  by a factor of 100 results in an increase of the degree of degradation by a factor of only 5. That means, as the absorbed dose is kept constant, the initial concentration of  $\text{PO}_2 \cdot$  undergoes only a little change. Thus, the increase of  $\text{O}_2$  causes a transition from  $v_g < v_i$  to  $v_g > v_i$ . The curves 3 and 4 in Figure 3 could then be interpreted by correlating the slowly decaying mode of the LSI decay to the decomposition of  $\text{PO}_2 \cdot$  or  $\text{P}_{\text{ox}} \cdot$ , as depicted by reactions (i) and (j), respectively. The respective rate constant is  $380 \text{ s}^{-1}$ . This conclusion is affirmed by the fact that the lifetime of the slowly decaying mode is

approaching a limiting value with increasing  $[\text{O}_2]$ , i.e., for a given dose the concentration of the oxidized species leading to main-chain scission has reached its maximum value, when all radicals  $\text{P} \cdot$  generated by that dose have reacted according to reaction (g). The relatively small portion of LSI decaying rapidly at high  $[\text{O}_2]$  is thought to be due to reaction (g) which is solely responsible for the LSI decay observable at low  $[\text{O}_2]$ , as is shown in Figure 3b. The straight line correlated to reaction (g) passes the transition range to the  $[\text{O}_2]$  range where reaction (i) is becoming rate determining.

**Acknowledgment.** The authors appreciated gratefully the assistance of Dr. G. Beck in running the lasers used during this work. The authors also are grateful to Professor J. K. Kochi for private discussions.

## References and Notes

- (1) T. R. Price and R. B. Fox, *J. Polym. Sci., Polym. Lett. Ed.*, **4**, 771 (1966).
- (2) S. W. Beavan, G. Beck, and W. Schnabel, *Eur. Polym. J.*, submitted.
- (3) G. Beck, J. Kiwi, D. Lindenau, and W. Schnabel, *Eur. Polym. J.*, **10**, 1069 (1974).
- (4) G. Beck, D. Lindenau, and W. Schnabel, *Eur. Polym. J.*, **11**, 761 (1975).
- (5) G. Dobrowolski, J. Kiwi, and W. Schnabel, *Eur. Polym. J.*, **12**, 657 (1976).
- (6) G. Beck, D. Lindenau, and W. Schnabel, *Macromolecules*, **10**, 135 (1977).
- (7) C. G. Hatchard and C. A. Parker, *Proc. R. Soc. London, Ser. A*, **235**, 518 (1956).
- (8) J. G. Calvert and J. N. Pitts, "Photochemistry", Wiley, New York, N.Y., 1967, p 781.
- (9) F. Fischer and G. Pfeleiderer, *Abh. Kenntnis Kohle*, **5**, 574 (1922).

## Kinetics of the Helix–Coil Transition of Polypeptides

Kazuo Ishiwari and Akio Nakajima\*

Department of Polymer Chemistry, Kyoto University, Sakyo-ku, Kyoto 606, Japan.  
Received February 14, 1978

**ABSTRACT:** The mean relaxation time of the peptide units in the helix–coil transition of a polypeptide was calculated by means of an extension of Glauber's dynamical theory of the one-dimensional Ising model. The critical slowing down is found near the transition midpoint for all units and is strong for the middle units of the chain. The mean relaxation time of the unit is dependent on the position of the unit in the chain. NMR spectra were simulated by use of the calculated mean relaxation times of the units. From comparison of the simulated NMR spectra with experiment, it is shown that the appearance of separate peaks of  $\alpha\text{-CH}$  in the NMR spectra is due to the polydispersity in molecular weight of the polypeptide sample.

Recently kinetics of the helix–coil transition of polypeptides has been studied both experimentally and theoretically. Unlike the situation for the equilibrium theory, the kinetics of the helix–coil transition is not well established. Previous theories<sup>1,2</sup> treat the initial rates of relaxation of the helical content by perturbation from equilibrium. The initial rate treatment has been widely and successfully used to interpret experimental data obtained by approach-to-equilibrium measurement, such as temperature jump,<sup>3</sup> ultrasonic absorption,<sup>4</sup> dielectric relaxation,<sup>5</sup> and yields relaxation times of the order of  $10^{-5}$ – $10^{-8} \text{ s}$  associated with the kinetics of the transition. On the other hand, high resolution nuclear magnetic resonance spectroscopy has been used to study the helix–coil transition under equilibrium conditions.<sup>6</sup> The NMR observation of separate peaks of  $\alpha\text{-CH}$  in the transition region, separated by chemical shift differences of the order of  $10^2 \text{ Hz}$ , implies the presence of lifetimes of about  $10^{-2} \text{ s}$  or greater.<sup>7</sup>

Though several workers<sup>8–12</sup> have investigated this contra-

diction in relaxation time, two theoretical models have been proposed to investigate this contradiction. Ullman,<sup>9</sup> Bradbury et al.,<sup>10</sup> and Nagayama and Wada<sup>11</sup> have explained the NMR peaks in terms of molecular weight polydispersity. On the other hand, Ferretti et al.<sup>7,11</sup> and Miller<sup>12</sup> have attributed this discrepancy to slow nucleation of helix units from random-coil polypeptide and concluded that the fast times by both experiments and theories are related to the time for adding to or melting one helix unit from an existing helical sequence and the slow time by NMR measurement is related to the formation of helix from random-coil polypeptide. The approach-to-equilibrium measurements investigate the relaxation of approach to new equilibrium of the helical content of the polypeptide chain when the system at equilibrium is perturbed. On the other hand, NMR measurement is concerned with more microscopic temporal states of individual peptide units under equilibrium conditions.

In this paper, we are concerned with the mean relaxation

time of individual peptide units and have investigated the dependence of the mean relaxation time on the position of the unit in the chain, from the point of view described above. Further, we simulated NMR spectra by use of the calculated mean relaxation times, and by comparing the simulated NMR spectra with experimental NMR spectra, we explore the origin of the separate peaks of  $\alpha$ -CH which appear in NMR spectra.

### Kinetics of the Helix-Coil Transition

Glauber<sup>13</sup> has presented a theory of the time-dependent one-dimensional Ising model for an infinitely long ferromagnet. In this section, we describe a model for the kinetics of the helix-coil transition of polypeptides of finite lengths in terms of the dynamics of the one-dimensional Ising model presented by Glauber.

The variable  $\mu_j$  describes the states of the  $j$ th unit as follows:

	ferromagnet	polypeptide
$\mu_j = +1$	parallel to magnetic field,	helix
$= -1$	antiparallel to magnetic field,	coil

(1)

The Hamiltonian (or free energy in the case of polypeptides) of the system is described as

$$\mathcal{H}\{\mu\} = -J \sum_{j=1}^{N-1} \mu_j \mu_{j+1} - H \sum_{j=1}^N \mu_j \quad (2)$$

where  $J$  is the cooperative interaction between adjacent units and  $H$  is related to the energy difference between two states of a unit. Glauber showed a transition probability, the probability per unit time that the  $j$ th unit makes a transition from the value  $\mu_j$  to  $-\mu_j$ , is given by the following equation according to the principle of detailed balance:

$$\omega_j(\mu_j) = \frac{k}{2} \left\{ 1 - \frac{\lambda}{2} \mu_j (\mu_{j-1} + \mu_{j+1}) \right\} (1 - \beta \mu_j) \quad (3)$$

where  $k$  is the rate constant at which the unit makes the transition from either state to the opposite one, whence  $k^{-1}$  is the time scale on which the transition takes place, and

$$\begin{aligned} \lambda &= \tanh(2J/k_B T) \\ \beta &= \tanh(H/k_B T) \end{aligned} \quad (4)$$

where  $k_B$  is Boltzmann's constant and  $T$  is the absolute temperature.

The parameters  $J$  and  $H$  can be related to the standard Zimm-Bragg parameters<sup>14</sup>  $s$  and  $\sigma$  in the theory of the helix-coil transition. By comparison of the free energy of the three-sequence state (1,1,1) with that of the state (-1,-1,-1), a relationship between  $H$  and  $s$  can be derived as  $s = \exp(2H/k_B T)$ . And by comparison of the free energy of the state (1,1,1) with that of the state (-1,-1,-1), and by the above relationship, a relationship between  $J$  and  $\sigma$  can be derived as  $\sigma = \exp(-4J/k_B T)$ . From the two above-mentioned relationships and eq 4,  $\lambda$  and  $\beta$  can be related to  $s$  and  $\sigma$  as follows:

$$\begin{aligned} \lambda &= (1 - \sigma)/(1 + \sigma) \\ \beta &= (s - 1)/(s + 1) \end{aligned} \quad (5)$$

The elemental steps of the kinetics of the helix-coil transition with nearest neighbor interaction are illustrated with the transition probabilities in Figure 1. On the other hand, Schwarz<sup>1</sup> introduced additional kinetic parameters  $\gamma_H$  and  $\gamma_C$  associated with the helix nucleation step and the coil nucleation step, respectively (see Figure 1). Though there is no knowledge about these parameters at the present, we will discuss the effect of these parameters on the mean relaxation time in a later section.

Since we consider polypeptides of finite lengths, the end

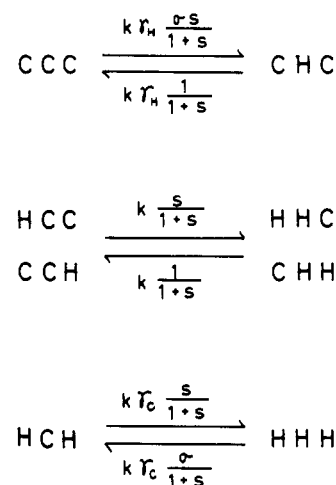


**Figure 1.** The transition probabilities between the states of a peptide unit. Helix is represented by H and coil by C.

effect has to be taken into consideration. In the equilibrium statics of the helix-coil transition, two phantom coil units, one to each end of the chain, are appended. Namely, the following boundary condition is given:

$$\mu_0 = \mu_{N+1} = -1 \quad (6)$$

This condition corresponds to the situation that the units near the chain end have less probability of being in a helix conformation than units near the center of the chain.

### Time Correlation Function and Relaxation Time of the Peptide Unit

Now we consider the normalized time correlation function of the  $j$ th unit

$$\Phi_j^i(t) = \frac{\langle \mu_i(0) \mu_j(t) \rangle - \langle \mu_i \rangle \langle \mu_j \rangle}{\langle \mu_i \mu_j \rangle - \langle \mu_i \rangle \langle \mu_j \rangle} \quad (7)$$

where angular brackets indicate the average over all conformations of a polypeptide. The mean relaxation time of the  $j$ th unit correlation,  $\tau_j$ , is given by

$$\tau_j = \int_0^\infty \Phi_j^i(t) dt \quad (8)$$

In order to calculate the integral of the right-hand side of eq 8, the Fourier-Laplace transform of the time correlation function is considered:

$$\Psi_j^i(\omega) = \int_0^\infty \Phi_j^i(t) \exp(-i\omega t) dt \quad (9)$$

And the mean relaxation time is given by eq 8 and 9:

$$\tau_j = \Psi_j^i(0) \quad (10)$$

Glauber showed that the time correlation function obeys the following equation:

$$-\frac{d}{dt} \langle \mu_i(0) \mu_j(t) \rangle = -2 \langle \mu_i(0) \mu_j(t) \omega_j(\mu_j(t)) \rangle \quad (11)$$

Substituting eq 3 into eq 11, we obtain

$$\begin{aligned} -\frac{1}{k} \frac{d}{dt} \langle \mu_i(0) \mu_j(t) \rangle &= \langle \mu_i(0) \mu_j(t) \rangle \\ &\quad - \frac{\lambda}{2} \{ \langle \mu_i(0) \mu_{j-1}(t) \rangle + \langle \mu_i(0) \mu_{j+1}(t) \rangle \} \\ &\quad + \frac{\beta \lambda}{2} \{ \langle \mu_i(0) \mu_{j-1}(t) \mu_j(t) \rangle + \langle \mu_i(0) \mu_j(t) \mu_{j+1}(t) \rangle \} \\ &\quad - \beta \langle \mu_i \rangle \end{aligned} \quad (12)$$

The differential equation of eq 12 is the coupled hierarchy equation, in which the third-order correlation function is needed to find the second-order correlation functions except when  $\beta = 0$  ( $s = 1$ ). In order to truncate the hierarchy equation, an approximation introduced by Tanaka et al.<sup>15</sup> was used:

$$\begin{aligned} \frac{\langle \mu_i(0) \mu_j(t) \mu_{j+1}(t) \rangle - \langle \mu_i \rangle \langle \mu_j \mu_{j+1} \rangle}{\langle \mu_i \mu_j \mu_{j+1} \rangle - \langle \mu_i \rangle \langle \mu_j \mu_{j+1} \rangle} \\ \simeq \frac{1}{2} \frac{\langle \mu_i(0) \mu_j(t) \rangle - \langle \mu_i \rangle \langle \mu_j \rangle}{\langle \mu_i \mu_j \rangle - \langle \mu_i \rangle \langle \mu_j \rangle} \\ + \frac{1}{2} \frac{\langle \mu_i(0) \mu_{j+1}(t) \rangle - \langle \mu_i \rangle \langle \mu_{j+1} \rangle}{\langle \mu_i \mu_{j+1} \rangle - \langle \mu_i \rangle \langle \mu_{j+1} \rangle} \quad (13) \end{aligned}$$

Equation 13 is exact at  $t = 0$  or  $t \rightarrow \infty$  (i.e., at equilibrium). For convenience sake, eq 13 is rewritten as follows:

$$\begin{aligned} \langle \mu_i(0) \mu_j(t) \mu_{j+1}(t) \rangle \simeq \langle \mu_i \rangle \langle \mu_j \mu_{j+1} \rangle \\ + \frac{1}{2} G_{j,j+1}^i \{ \langle \mu_i(0) \mu_j(t) \rangle - \langle \mu_i \rangle \langle \mu_j \rangle \} \\ + \frac{1}{2} G_{j,j+1}^i \{ \langle \mu_i(0) \mu_{j+1}(t) \rangle - \langle \mu_i \rangle \langle \mu_{j+1} \rangle \} \quad (14) \end{aligned}$$

where

$$G_{j,k}^i = \frac{\langle \mu_i \mu_j \mu_{j+1} \rangle - \langle \mu_i \rangle \langle \mu_j \mu_{j+1} \rangle}{\langle \mu_i \mu_k \rangle - \langle \mu_i \rangle \langle \mu_k \rangle} \quad (15)$$

Using this approximation, eq 12 is linearized for

$$\phi_j^i(t) = \langle \mu_i(0) \mu_j(t) \rangle - \langle \mu_i \rangle \langle \mu_j \rangle \quad (16)$$

as:

$$\begin{aligned} -\frac{1}{k} \frac{d}{dt} \phi_1^i(t) &= a_1^i \phi_1^i(t) - \frac{\lambda}{2} c_1^i \phi_1^i(t) \\ -\frac{1}{k} \frac{d}{dt} \phi_j^i(t) &= a_j^i \phi_j^i(t) - \frac{\lambda}{2} \{ b_j^i \phi_{j-1}^i(t) + c_j^i \phi_{j+1}^i(t) \} \\ -\frac{1}{k} \frac{d}{dt} \phi_N^i(t) &= a_N^i \phi_N^i(t) - \frac{\lambda}{2} b_N^i \phi_{N-1}^i(t) \quad (17) \end{aligned}$$

where

$$\begin{aligned} a_1^i &= 1 - \frac{\beta\lambda}{2} (1 - \frac{1}{2} G_{1,1}^i) \\ a_j^i &= 1 + \frac{\beta\lambda}{4} (G_{j-1,j}^i + G_{j,j}^i) \quad (2 \leq j \leq N-1) \\ a_N^i &= 1 - \frac{\beta\lambda}{2} (1 - \frac{1}{2} G_{N-1,N}^i) \\ b_j^i &= 1 - \frac{\beta}{2} G_{j-1,j-1}^i \\ c_j^i &= 1 - \frac{\beta}{2} G_{j,j+1}^i \quad (18) \end{aligned}$$

In eq 17, it is considered that  $\phi_j^i(t) \rightarrow 0$  at  $t \rightarrow \infty$  (i.e.,  $\lim_{t \rightarrow \infty} \langle \mu_i(0) \mu_j(t) \rangle = \langle \mu_i \rangle \langle \mu_j \rangle$ ).

This set of coupled differential equations can be rewritten in terms of the Fourier–Laplace transform.

$$\psi_j^i(\omega) = \int_0^\infty \phi_j^i(t) \exp(-i\omega t) dt \quad (19)$$

To avoid complexity, upper suffix  $i$  is omitted below. Then it can be shown that

$$\psi_j^i(\omega) = \frac{2}{k\lambda} \sum_{k=1}^N M_{j,k}^{-1}(\omega) \phi_k(0) \quad (20)$$

where  $M_{j,k}^{-1}$  is the  $(j,k)$  element of matrix  $\mathbf{M}^{-1}$ , where  $\mathbf{M}$  is an  $N \times N$  matrix

$$\mathbf{M} = \begin{pmatrix} 2\epsilon_1 & -c_1 & 0 & 0 & \dots \\ -b_1 & 2\epsilon_2 & -c_2 & 0 & \dots \\ 0 & -b_3 & 2\epsilon_3 & -c_3 & \dots \\ & & \dots & 2\epsilon_{N-1} & -c_{N-1} \\ & & & -b_N & 2\epsilon_N \end{pmatrix} \quad (21)$$

where

$$\epsilon_j = (1/\lambda)[a_j + i(\omega/k)] \quad (22)$$

Initial conditions  $\phi_k(0)$  and  $G_{j,k}^i$  are given by the static correlation function calculated by statistical mechanics of the helix–coil transition and presented briefly in the Appendix. Let  $D_i$  be the determinant of the  $i \times i$  matrix obtained from the first  $i$  rows and columns of matrix  $\mathbf{M}$  and  $E_i$  be the determinant of the  $i \times i$  matrix obtained from  $\mathbf{M}$  after elimination of the first  $N-i$  rows and columns, thus

$$D_0 = 1$$

$$D_1 = 2\epsilon_1$$

$$D_i = 2\epsilon_i D_{i-1} - b_i c_{i-1} D_{i-2} \quad (2 \leq i \leq N) \quad (23)$$

$$E_0 = 1$$

$$E_1 = 2\epsilon_N$$

$$E_i = 2\epsilon_{N-i+1} E_{i-1} - b_{N-i+2} c_{N-i+1} E_{i-2} \quad (2 \leq i \leq N) \quad (24)$$

Using  $D_i$  and  $E_i$  defined above

$$\begin{aligned} M_{j,k}^{-1} &= \left( \prod_{m=k+1}^j b_m \right) \frac{D_{k-1} E_{N-j}}{D_N}, \quad j > k \\ M_{j,k}^{-1} &= \frac{D_{j-1} E_{N-j}}{D_N}, \quad j = k \\ M_{j,k}^{-1} &= \left( \prod_{m=j}^{k-1} c_m \right) \frac{D_{j-1} E_{N-k}}{D_N}, \quad j < k \end{aligned} \quad (25)$$

The mean relaxation time of the  $j$ th unit is given by

$$\tau_j = \Psi_j^j(0) = \frac{\psi_j^j(0)}{1 - \langle \mu_j \rangle^2} \quad (26)$$

If chain length is infinite,  $\langle \mu_j \rangle$ ,  $G_{j,k}^i$ ,  $a_j^i$ ,  $b_j^i$ , and  $c_j^i$  are independent of  $i$ ,  $j$ , and  $k$  and equations are rewritten as follows:

$$\begin{aligned} \langle \mu_j \rangle &= \mu \\ G_{j,k}^i &= G \\ a_j^i &= 1 + (\beta\lambda/2)G = a \\ b_j^i &= 1 - (\beta/2)G = b \\ c_j^i &= 1 - (\beta/2)G = b \quad (27) \end{aligned}$$

(see Appendix). The coupled differential equation (i.e., eq 17) becomes as follows:

$$-\frac{1}{k} \frac{d}{dt} \phi_j^i(t) = a \phi_j^i(t) - \frac{\lambda}{2} \{ b \phi_{j-1}^i(t) + \phi_{j+1}^i(t) \} \quad (28)$$

According to Glauber's procedure,  $\phi_j^i(t)$  can be described as

$$\begin{aligned} \phi_j^i(t) &= \exp(-ka) \sum_{k=-\infty}^{\infty} \phi_k^i(0) I_{j-k}(\lambda k b t) \\ &= \exp(-ka) \sum_{k=-\infty}^{\infty} (1 - \mu^2) \chi^{|i-j+k|} I_k(\lambda k b t) \quad (29) \end{aligned}$$

where  $I_k(x)$  is the Bessel function of imaginary argument and

$$\chi = (1 + s - [(1-s)^2 + 4\sigma s]^{1/2}) / (1 + s + [(1-s)^2 + 4\sigma s]^{1/2}) \quad (30)$$

(see Appendix). The Fourier–Laplace transform of eq 29 can be done exactly, and when  $i = j$ , the result is

$$\begin{aligned} \frac{\psi_j^j(\omega)}{1 - \mu^2} = \Psi_j^j(\omega) &= \frac{1}{k\lambda(\epsilon^2 - b^2)^{1/2}} \\ &\times \frac{1 + b\chi/(\epsilon + (\epsilon^2 - b^2)^{1/2})}{1 - b\chi/(\epsilon + (\epsilon^2 - b^2)^{1/2})} \quad (31) \end{aligned}$$

where

$$\epsilon = (1/\lambda)(a + i(\omega/k))$$

When  $s = 1$ ,  $\mu = G = 0$  and  $a = b = 1$ , therefore the mean relaxation time  $\tau$  is given by

$$\tau = \psi_j^i(0) = (1 + \sigma)^2/4\sigma k \simeq (4\sigma k)^{-1} \quad (\text{at } s = 1) \quad (32)$$

This result is equal to the Schwarz's result,<sup>1</sup> though the relaxation time defined by eq 8 in this paper has different meaning from that defined by Schwarz.

### Simulation of NMR Spectra

Tanaka et al.<sup>15</sup> derived a time correlation function of the nuclear spin of a peptide unit  $M_j(t)$ ,  $P_j(t)$ , as

$$\begin{aligned} P_j(t) &= \frac{\langle M_j^*(0)M_j(t) \rangle}{\langle M_j^*M_j \rangle} \\ &= \exp\left(-\frac{p_{j,h}\alpha_h + p_{j,c}\alpha_c}{2}t\right) \\ &\quad \times \left\langle \exp\left[\frac{\alpha_c - \alpha_h}{2} \int_0^t \Delta\mu_j(t') dt'\right] \right\rangle \quad (33) \end{aligned}$$

where  $\alpha_h = -i\omega_h + T_h^{-1}$ ,  $\alpha_c = -i\omega_c + T_c^{-1}$  ( $T_h$  and  $T_c$  are the relaxation times, associated with protons in helical state and coil state, respectively)  $\Delta\mu_j(t) = \mu_j(t) - \langle \mu_j \rangle$ , and  $p_{j,h} = (1 + \langle \mu_j \rangle)/2$  and  $p_{j,c} = (1 - \langle \mu_j \rangle)/2$  (the probabilities that the unit is in helical and coil state, respectively).

By assuming that  $\mu_j(t)$  is a Gaussian process,<sup>16</sup>  $P_j(t)$  is described as

$$\begin{aligned} P_j(t) &= \exp\left(-\frac{p_{j,h}\alpha_h + p_{j,c}\alpha_c}{2}t\right) \\ &\quad \times \exp\left[-\left|\frac{\alpha_c - \alpha_h}{2i}\right|^2 \langle (\Delta\mu_j)^2 \rangle \right. \\ &\quad \left. \times \int_0^t (t-t')\Phi_j(t') dt'\right] \quad (34) \end{aligned}$$

where  $\Phi_j(t)$  is  $\Phi_j^i(t)$  in eq 7. If the following inequality is satisfied,

$$\eta_j = \left|\frac{\alpha_c - \alpha_h}{2i}\right| \langle (\Delta\mu_j)^2 \rangle^{1/2} \tau_j \ll 1 \quad (35)$$

in other words, if the relaxation time of the helix-coil transition of a peptide unit is much less than that of the proton nuclear spin of the unit, the time correlation function  $p_j(t)$  can be described as

$$P_j(t) = \exp\left[-\eta_j^2 \left(\frac{t}{\tau_j} - 1\right) - (p_{j,h}\alpha_h + p_{j,c}\alpha_c)t\right] \quad (36)$$

Therefore, the line shape of the NMR spectra of the  $j$ th unit is given by

$$\begin{aligned} I_j(\omega) &= \frac{1}{\pi} \text{Re} \left[ \int_0^\infty P_j(t) \exp(-i\omega t) dt \right] \\ &= \frac{\exp(\eta_j^2)}{\pi} \\ &\quad \times \frac{\eta_j^2/\tau_j + p_{j,h}T_h^{-1} + p_{j,c}T_c^{-1}}{(\omega - \omega_{\text{obsd}})^2 + (\eta_j^2/\tau_j + p_{j,h}T_h^{-1} + p_{j,c}T_c^{-1})^2} \quad (37) \end{aligned}$$

where  $\omega_{\text{obsd}} = p_{j,h}\omega_h + p_{j,c}\omega_c$ . The approximations used in order to derive eq 37 are that  $\mu_j(t)$  is a Gaussian process, the relaxation time of the helix-coil transition of a peptide unit is much less than that of the proton nuclear spin of the unit, and the time correlation function,  $\Phi_j(t)$ , is approximated in terms of the mean relaxation time  $\tau_j$ , i.e.,  $\Phi_j(t) \simeq \exp(-t/\tau_j)$ .

The total line shape of the NMR spectra is given by

$$I(\omega) = \sum_{j=1}^N I_j(\omega) \quad (38)$$

### Results and Discussion

**The Mean Relaxation Time.** We indicate the calculated mean relaxation times in the form of the reduced mean relaxation times,  $k\tau_j$ . In order to calculate the reduced mean relaxation time, the  $\sigma$  values must be specified. In various mixed organic solvent systems for various polypeptides, the  $\sigma$  value is of the order of  $10^{-4}$ . Therefore  $10^{-4}$  was employed as the  $\sigma$  value in this study.

The calculated mean relaxation time of given units is shown as a function of  $s$  for a chain of 41 units in Figure 2. The critical slowing down is observed, i.e., the mean relaxation time has a maximum near the transition mid point  $s_m$  (at which time the helical content,  $\theta$ , is 0.5). For a middle unit of the chain the critical slowing down is especially to be noted. Actually, since  $s_m$  for a chain of 41 units is 1.18, the mean relaxation time has a maximum at a somewhat smaller  $s$  than  $s_m$ . The middle unit  $s$  at which the relaxation time has a maximum,  $s_c$ , is equal to  $s_m$ . However,  $s_c$  for the unit near the chain end is smaller than for the unit near the center of the chain.

The position dependence of the mean relaxation time for several  $s$  values is shown in Figure 3 for a chain of 41 units. The mean relaxation time strongly depends on the position of the unit in the chain especially for  $s$  values nearly equal to  $s_m$ . The mean relaxation time of a unit located near the center of the chain is much larger than that of a unit located near the chain end. The helix-coil transition of a short chain can be described by one helix-region model, in which the chain has one helix sequence restricted to the interior of the chain, so diffusion of the two helix-coil boundaries (propagation steps in our words) dominates the kinetics of the transition and the nucleation step rarely occurs. Therefore a unit located near the center of the chain has a much larger mean relaxation time.

In Figure 4, the mean relaxation times of given units for a chain of 81 units are shown as functions of  $s$ . The same behavior as that for a chain of 41 units can be seen. The maximum value of the mean relaxation time for the middle unit is smaller for a shorter chain than for a longer chain. On the other hand, the maximum value of the mean relaxation time of the unit located at the same position from the chain end is larger for a shorter chain than for a longer chain.

As described in the previous section, Schwarz<sup>1</sup> introduced additional kinetic parameters  $\gamma_H$  and  $\gamma_C$  associated with the rate constants of helix nucleation and coil nucleation, respectively. Here we consider the case in which  $\gamma_H = \gamma_C = \gamma$ . In such a case, the transition probability,  $\omega_j(\mu_j)$ , is given by

$$\omega_j(\mu_j) = \frac{k'}{2} \left\{ 1 + \delta\mu_{j-1}\mu_{j+1} - \frac{\lambda'}{2} \mu_j(\mu_{j-1} + \mu_{j+1}) \right\} (1 - \beta\mu_j) \quad (39)$$

where

$$\begin{aligned} k' &= \frac{\gamma\sigma + \gamma + 2}{4} k \\ \delta &= \frac{\gamma\sigma + \gamma - 2}{\gamma + \gamma + 2} \\ \lambda' &= \frac{2\gamma(1 - \sigma)}{\gamma\sigma + \gamma + 2} \quad (40) \end{aligned}$$

If  $\gamma$  is  $2/(1 + \sigma)$ , then  $k' = k$ ,  $\delta = 0$ , and  $\lambda' = \lambda$ , and eq 39 becomes equivalent to eq 3. Namely this value is  $2/(1 + \sigma) = 2/[1 + \exp(-4J/k_B T)]$  in the dynamics of the Ising model by Glauber. The assumption that  $\gamma$  is equal to  $2/(1 + \sigma)$  corresponds to the assumption that the transition  $(-1, 1, -1) \rightarrow$

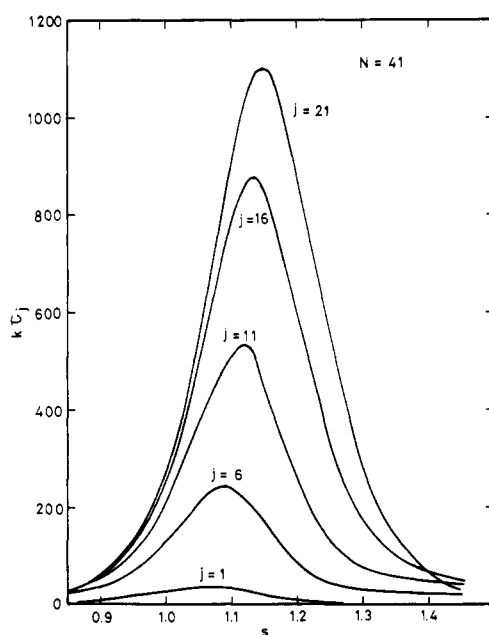


**Figure 2.** Reduced mean relaxation time as a function of  $s$  for different units in a chain of 41 units. A value of  $\sigma = 10^{-4}$  was chosen.

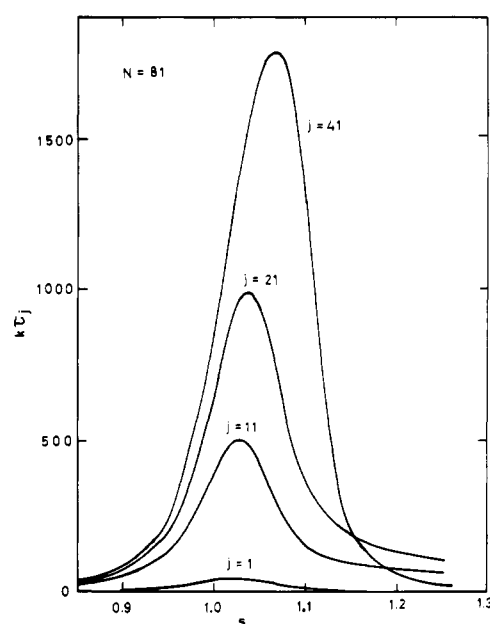


**Figure 4.** Reduced mean relaxation time as a function of  $s$  for different units in a chain of 81 units.

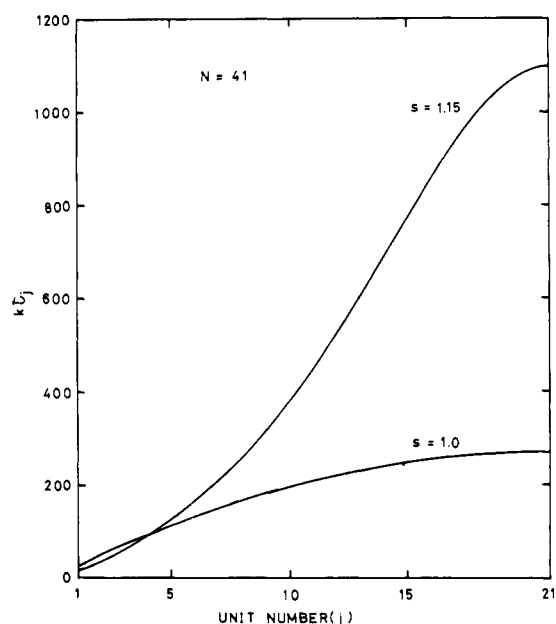


**Figure 3.** Reduced mean relaxation time as a function of position of the unit in a chain of 41 units.

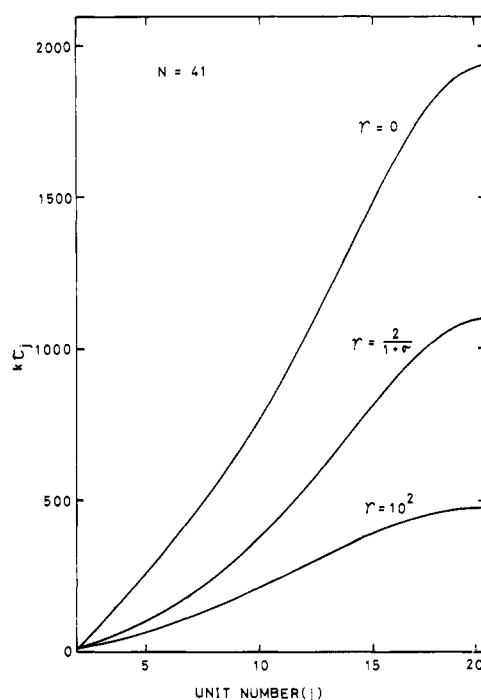


**Figure 5.** Position dependence of the reduced mean relaxation time for different  $\gamma$  values in a chain of 41 units.

$(-1, -1, -1)$  (or  $(1, -1, 1) \rightarrow (1, 1, 1)$ ) occurs twice as fast as the transition  $(-1, 1, 1) \rightarrow (-1, -1, 1)$  (or  $(1, -1, -1) \rightarrow (1, 1, -1)$ ) since  $\sigma \approx 0$  and  $\gamma \approx 2$ . This is due to the situation that the helix unit that makes the transition to coil is bounded by two adjacent coil units in the transition  $(-1, 1, -1) \rightarrow (-1, -1, -1)$ , while the helix unit is bounded by one coil unit on one side in the transition  $(-1, 1, 1) \rightarrow (-1, -1, 1)$ . The mean relaxation time of the middle unit of a chain of 41 units as a function of  $s$  is shown for various  $\gamma$  values in Figure 5. In Figure 6, the mean relaxation time of the middle unit in the chain of the same length is shown as a function of  $\gamma$  for different  $s$  values. As shown in Figures 5 and 6, the mean relaxation time is larger for a small  $\gamma$  value than for a bigger  $\gamma$  value. In the case in which  $\gamma$  is small, the nucleation step rarely occurs and the propagation step is significant in the transition. Therefore the mean relaxation time becomes larger and the

position dependence of the mean relaxation time is stronger for a small  $\gamma$  value. Though the mean relaxation time is dependent on  $\gamma$  as described above, its order of magnitude does not change even in the case of zero  $\gamma$ . In other words, the dependence on  $\gamma$  is not so strong in the case of a short chain. For such short polypeptides, the one helix-region model is valid, and the nucleation step rarely occurs, as described in the previous section.  $\gamma = 0$  corresponds to the one helix-region model in the kinetics of the transition. Therefore the mean relaxation time does not strongly depend on  $\gamma$  for such a short chain. In Figure 7, the position dependence of the mean relaxation time for chains of different lengths is shown for  $s = 1.0$  and  $\gamma = 0$ . Strong position dependence is shown.

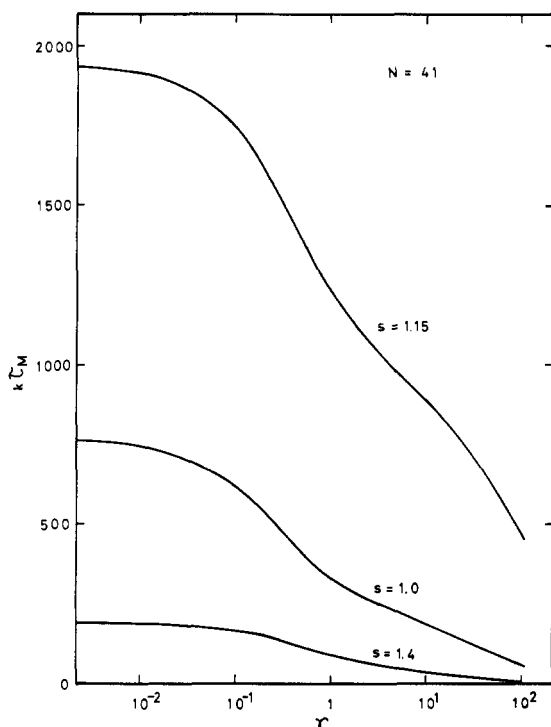


Figure 6. Reduced mean relaxation time of the middle unit in a chain of 41 units as a function of the  $\gamma$  value for different  $s$  values.

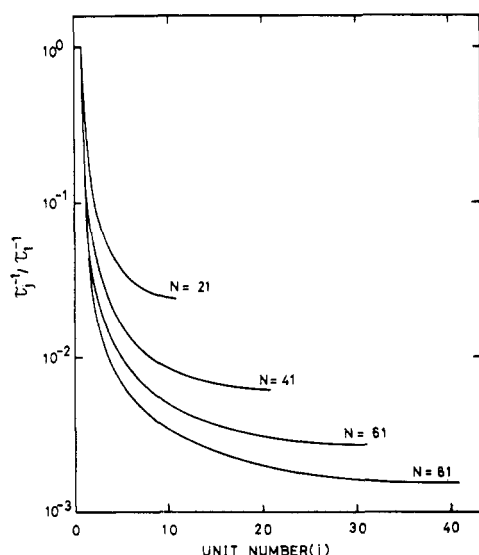


Figure 7. Ratio of the inverse of the mean relaxation time of the  $j$ th unit to the inverse of the mean relaxation time of the first unit at  $s = 1.0$  with different degrees of polymerization in the case of  $\gamma = 0$ .

**Nuclear Magnetic Resonance Spectra.** In order to estimate the absolute value of the mean relaxation time  $\tau_j$ , the  $k$  value must be specified. Recently Zana<sup>17</sup> summarized published results of the relaxation time and by substituting these values into the Schwarz equation (eq 32) he concluded that the most probable value of the rate constant for the elemental step of helix growth is about  $10^8 \text{ s}^{-1}$ . He thought that the elemental step of helix growth appears to be limited by the rate of rotation of short segments of the polypeptide chain around C-C' and C-N bonds. If  $10^8 \text{ s}^{-1}$  is adopted to the  $k$  value the mean relaxation time of the peptide unit is of the order of  $10^{-5} \text{ s}$  even in the case in which  $\gamma$  is zero. Because of this result and the fact that the chemical shift difference in 220-MHz NMR is about  $10^2 \text{ Hz}$ , the inequality of eq 35 is satisfied.

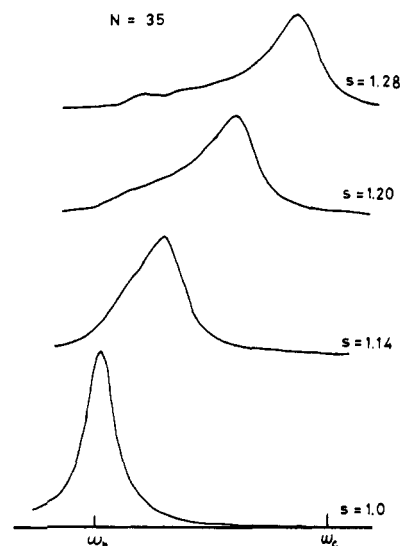


Figure 8. Simulated NMR spectra for a chain of 35 units with  $\sigma = 10^{-4}$ ,  $T_h^{-1} = 11.75 \text{ s}^{-1}$ ,  $T_c^{-1} = 10.75 \text{ s}^{-1}$ , and a chemical shift difference of 134 Hz.<sup>11</sup>

To simulate the NMR spectra,  $\omega_h$ ,  $\omega_c$ ,  $T_h$ , and  $T_c$  must be specified, where  $\omega_h$  and  $\omega_c$  are the chemical shifts and  $T_h$  and  $T_c$  are the relaxation times associated with protons in helical and coil state, respectively. These values were taken from the 220-MHz NMR data of Nagayama and Wada<sup>11</sup> for a fairly monodisperse sample of 35 units. Namely,  $\omega_h - \omega_c = 134 \text{ Hz}$ ,  $T_h^{-1} = 11.75 \text{ s}^{-1}$ , and  $T_c^{-1} = 10.75 \text{ s}^{-1}$ .

In Figure 8, the simulated NMR spectra calculated by use of eq 37 and 38 is shown for a chain of 35 units. A small shoulder and a very small peak near the coil resonance at high helical constant region are indicated. This shoulder and peak are the result of the fact that the units located near the chain end have less probability of being in helical conformation than the units near the center of the chain. The end effect is essential to the appearance of separate peaks of polydisperse sample.

The line shape of a polydisperse sample, in which the number fraction of  $p$ -mer is  $f_p$ , is given by

$$I(\omega) = \sum_p f_p I_p(\omega) \quad (41)$$

In Figure 9, the simulated and experimental NMR spectra of the polydisperse sample are shown, in which the molecular weight distribution is similar to that of the sample used in NMR measurements by Milstien and Ferretti<sup>18</sup> and Ferretti and Jernigan.<sup>7</sup> In both the simulated and the experimental spectra, the coil and helix peaks are shown; the coil peak does not shift and the helix peak only shifts slightly. Even at the high helical content region, a small coil peak still exists in both spectra. Though the third peak is shown between helix and coil peaks in the simulated spectra, this third peak seems to be partly due to the fact that the molecular weight distribution used in simulation is not a continuous function and the fraction is taken stepwise for each ten units.

In Figures 10 and 11, the simulated and experimental (in Figure 11) NMR spectra of longer samples are shown, in which the type of molecular weight distribution is the same as that of Figure 9. Though the molecular weight distributions of the samples in Figures 10 and 11 are unknown, it is hard to think that the distribution is narrower than for the shorter chain of the sample in Figure 9. Both helix and coil peaks are indicated, and the coil peak does not shift appreciably but merely changes intensity as in the case of the short chain. On the other hand, the helix peak shifts toward the coil peak. The shift of

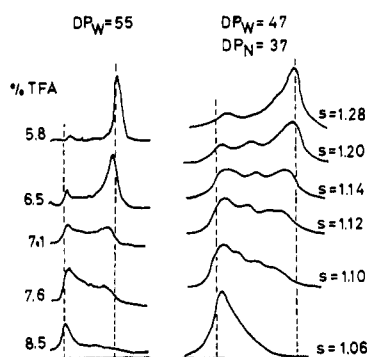


**Figure 9.** Simulated (right side) NMR spectra for a molecular weight polydisperse sample of  $DP_W = 47$  and  $DP_N = 37$ . Assumed molecular weight distribution is similar to that of the sample used in the NMR measurement of poly( $\gamma$ -benzyl L-glutamate) by Ferretti and Jernigan<sup>7</sup> and by Milstien and Ferretti.<sup>18</sup> Left-side spectra are the observed  $\alpha$ -CH spectra of poly( $\gamma$ -benzyl L-glutamate) ( $DP_W = 55$ ) by Ferretti and Jernigan.<sup>7</sup>

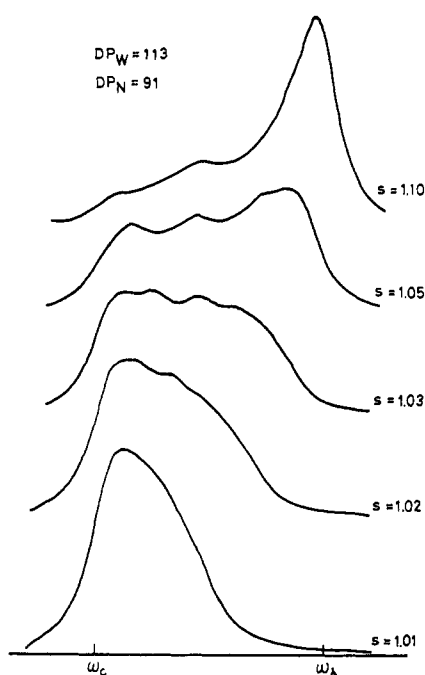


**Figure 10.** Simulated NMR spectra for a molecular weight polydisperse samples of  $DP_W = 113$  and  $DP_N = 91$ . The molecular weight distribution is the same as that in Figure 9.

the helix peak is more remarkable and the appearance of separate peaks is less clear in longer chain than in shorter chain. On the whole, the agreement between the simulated and experimental spectra is good as shown in Figures 9 and 11. Moreover the third peak that appears in the simulated spectra of short chain is not so distinct in that of the long chain. This seems to be due to the fact that the influence of discontinuity of the assumed molecular weight distribution is smaller in the longer chain, because the transition behavior is less dependent on molecular weight in longer chains than in shorter chains.

In Figure 12, the simulated NMR spectra of the narrower molecular weight distribution sample is shown, in which the distribution is similar to that of the monodisperse sample used by Milstien and Ferretti.<sup>18</sup> Coil and helix peaks are still shown in the fairly monodisperse sample, though the separation of the peaks is incomplete.

Consideration must be given to the molecular weight po-

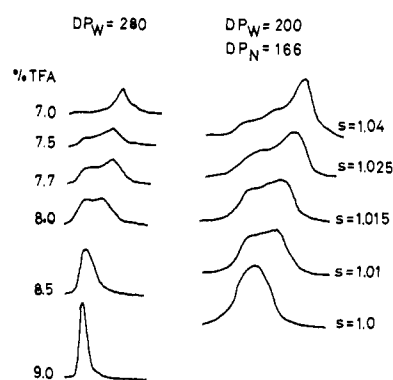


**Figure 11.** Similar to Figure 9 except for chain length.

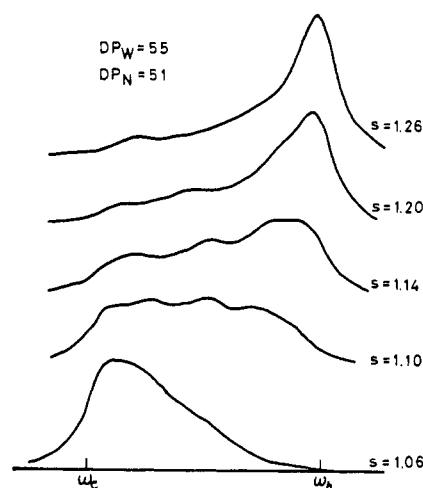


**Figure 12.** Simulated NMR spectra of a narrower molecular weight distribution sample of  $DP_W = 55$  and  $DP_N = 51$ . The distribution is similar to that of the sample used as a monodisperse sample by Milstien and Ferretti.<sup>18</sup>

lydispersity because it is unavoidable in the synthesized polymer. When the polydispersity is taken into consideration, the agreement between the simulated and experimental NMR spectra is good for both short chain and long chain as shown in this section. Further, recently we have shown that the separate peaks cannot be attributed to the long lifetime of the helix-coil transition of the order of  $10^{-2}$  s.<sup>19</sup> Therefore it is concluded that the separate peaks in the NMR spectra result from the molecular weight polydispersity of the sample.

There may be many kinds of relaxation modes in the helix-coil transition, some of which are not expected by the dynamics of the one-dimensional Ising model. For example, Fujiwara and Saito<sup>20</sup> have proposed theoretically the mode having a long time scale associated with helix nucleation from a completely helical polypeptide in order to explain the results of the isotope exchange experiments by Ikegami et al.<sup>21</sup> However, it is hard to think that the mode associated with coil nucleation has a much longer time scale than that associated with propagation step, as shown in our previous paper.<sup>19</sup> Therefore, it is concluded that both approach-to-equilibrium measurement and NMR measurement observe the same mode of the relaxation of the helix-coil transition.

## Appendix

In order to get the initial value of the time correlation function  $\phi_i^j(0)$  and  $G_{ij}^k$  factor, the correlation function at equilibrium is necessary. These are calculated on the base of the equilibrium statistical mechanics of the helix-coil tran-

sition. The procedure of calculation is the same as that of Tanaka and Suzuki.<sup>22</sup> However, all random-coil conformation is regarded as the energy standard in this study, and our transition matrix  $\mathbf{W}$  is

$$\mathbf{W} = \begin{vmatrix} s & \sigma^{1/2}s^{1/2} \\ \sigma^{1/2}s^{1/2} & 1 \end{vmatrix} \quad (\text{A1})$$

The partition function  $Z_N$  is given by

$$Z_N = \mathbf{e} \mathbf{W}_1 \mathbf{W}^{N-1} \mathbf{W}_N \mathbf{e}^+ \quad (\text{A2})$$

where

$$\mathbf{W}_1 = \begin{vmatrix} 0 & 0 \\ \sigma^{1/2}s^{1/2} & 1 \end{vmatrix}$$

$$\mathbf{W}_N = \begin{vmatrix} 0 & \sigma^{1/2}s^{1/2} \\ 0 & 1 \end{vmatrix}$$

$$\mathbf{e} = (1, 1) \text{ and } \mathbf{e}^+ = (1, 1)^+ \quad (\text{A3})$$

The correlation function is given as follows:

$$\langle \mu_i \mu_j \dots \mu_k \rangle = Z_N^{-1} \mathbf{e} \mathbf{W}_1 \mathbf{W}^{j-i} \mathbf{W}' \mathbf{W}^{k-j} \mathbf{W}' \dots \mathbf{W}' \mathbf{W}^{N-k} \mathbf{W}_N \mathbf{e}^+ \quad (\text{A4})$$

where

$$\mathbf{W}' = \begin{vmatrix} 1 & 0 \\ 0 & -1 \end{vmatrix} \quad (\text{A5})$$

For infinitely long polypeptide, the end effect does not have to be taken into consideration. Therefore

$$\langle \mu_i \rangle = \mu = \lim_{N \rightarrow \infty} \frac{\text{trace } \mathbf{W}^{i-1} \mathbf{W}' \mathbf{W}^{N-i}}{\text{trace } \mathbf{W}^{N-1}} \quad (\text{A6})$$

By transforming  $\mathbf{W}$  into diagonal matrix  $\Lambda$ , we get

$$\mu = \lim_{N \rightarrow \infty} \frac{\text{trace } \mathbf{T}^{-1} \Lambda^{i-1} \mathbf{T} \mathbf{W}' \mathbf{T}^{-1} \Lambda^{N-i} \mathbf{T}}{\text{trace } \mathbf{T}^{-1} \Lambda^{N-1} \mathbf{T}}$$

$$= \lim_{N \rightarrow \infty} \frac{\text{trace } \Lambda^{N-1} \mathbf{T} \mathbf{W}' \mathbf{T}^{-1}}{\text{trace } \Lambda^{N-1}} \quad (\text{A7})$$

where

$$\mathbf{W} = \mathbf{T}^{-1} \Lambda \mathbf{T} \quad (\text{A8})$$

and

$$\Lambda = \begin{vmatrix} \lambda_1 & 0 \\ 0 & \lambda_2 \end{vmatrix} \quad (\text{A9})$$

where  $\lambda_1$  and  $\lambda_2$  ( $\lambda_1 > \lambda_2$ ) are the eigenvalues of matrix  $\mathbf{W}$ .

$$\lambda_{1,2} = [1 + s \pm ((1-s)^2 + 4\sigma s)^{1/2}]/2 \quad (\text{A10})$$

By substituting  $\mathbf{T}^{-1}$  and  $\mathbf{T}$  calculated by eq A8 into eq A7, we get the following final result:

$$\mu = \frac{s-1}{\lambda_1 - \lambda_2} = \frac{s-1}{((1-s)^2 + 4\sigma s)^{1/2}} \quad (\text{A11})$$

The second-order correlation function  $\langle \mu_i \mu_j \rangle$  and  $G$  factor are also given by the same procedure, and the final results are

$$\frac{\langle \mu_i \mu_j \rangle - \langle \mu_i \rangle \langle \mu_j \rangle}{\langle \mu_i^2 \rangle - \langle \mu_i \rangle^2} = \frac{\langle \mu_i \mu_j \rangle - \mu^2}{1 - \mu^2} = \left( \frac{\lambda_2}{\lambda_1} \right)^{|i-j|} \quad (\text{A12})$$

( $\lambda_2/\lambda_1$ ) is equal to  $\chi$  in eq 29, and

$$G = \frac{\langle \mu_i \mu_j \mu_{j+1} \rangle - \langle \mu_i \rangle \langle \mu_j \mu_{j+1} \rangle}{\langle \mu_i \mu_j \rangle - \langle \mu_i \rangle \langle \mu_j \rangle} = \mu(1 - \chi) \quad (\text{A13})$$

## References and Notes

- (1) G. Schwarz, *J. Mol. Biol.*, **11**, 64 (1965).
- (2) D. Poland and H. A. Scheraga, *J. Chem. Phys.*, **45**, 2071 (1966).
- (3) R. Lumry, R. Legare, and W. G. Miller, *Biopolymers*, **2**, 486 (1964).
- (4) A. Barksdale and J. Stuehr, *J. Am. Chem. Soc.*, **94**, 3334 (1972); R. Zana and J. Lang, *Biopolymers*, **12**, 79 (1973).
- (5) G. Schwarz and J. Seeling, *Biopolymers*, **6**, 1263 (1968); A. Wada, T. Tanaka, and H. Kihara, *ibid.*, **11**, 587 (1972).
- (6) J. L. Markely, D. H. Meadows, and O. Jardetzky, *J. Mol. Biol.*, **27**, 25 (1967); W. E. Stewart, L. Mandelkern, and R. E. Glick, *Biochemistry*, **6**, 143 (1967); E. M. Bradbury, C. Crane-Robinson, L. Paolillo, and P. Temussi, *J. Am. Chem. Soc.*, **95**, 1683 (1973).
- (7) J. A. Ferretti and L. Paolillo, *Biopolymers*, **7**, 155 (1969); J. A. Ferretti and B. W. Ninham, *Macromolecules*, **3**, 30 (1970); J. A. Ferretti and R. L. Jernigan, *ibid.*, **6**, 687 (1973).
- (8) J. H. Bradbury and M. D. Fenn, *Aust. J. Chem.*, **22**, 357 (1969); J. W. O. Tam and I. M. Klotz, *J. Am. Chem. Soc.*, **93**, 1313 (1971); F. J. Joubert, N. Lotan, and H. A. Scheraga, *Biochemistry*, **9**, 2197 (1970); M. Goodman and N. Ueyama, *Biopolymers*, **12**, 2639 (1973).
- (9) R. Ullman, *Biopolymers*, **9**, 471 (1970).
- (10) E. M. Bradbury, C. Crane-Robinson, and H. W. E. Rattle, *Polymer*, **11**, 277 (1970); E. M. Bradbury, P. Cray, C. Crane-Robinson, L. Paolillo, T. Tancredi, and P. A. Temussi, *J. Am. Chem. Soc.*, **93**, 5916 (1971).
- (11) K. Nagayama and A. Wada, *Biopolymers*, **12**, 2443 (1973); **14**, 2489 (1975).
- (12) W. G. Miller, *Macromolecules*, **6**, 100 (1973).
- (13) R. J. Glauber, *J. Math. Phys.*, **4**, 294 (1963).
- (14) B. H. Zimm and J. K. Bragg, *J. Chem. Phys.*, **31**, 526 (1959).
- (15) T. Tanaka, A. Wada, and M. Suzuki, *J. Chem. Phys.*, **59**, 3799 (1973).
- (16) S. Chandrasekhar, *Rev. Mod. Phys.*, **15**, 1 (1943).
- (17) R. Zana, *Biopolymers*, **14**, 2425 (1975).
- (18) J. B. Miltien and J. A. Ferretti, *Biopolymers*, **12**, 2335 (1973).
- (19) K. Ishiwari and A. Nakajima, *Polym. J.*, in press.
- (20) M. Fujiwara and N. Saito, *Polym. J.*, **9**, 625 (1977).
- (21) M. Nakanishi, M. Tsuboi, A. Ikegami, and M. Kanehisa, *J. Mol. Biol.*, **64**, 363 (1972).
- (22) T. Tanaka and M. Suzuki, *J. Chem. Phys.*, **59**, 3795 (1973).